Acta Oceanol. Sin., 2024, Vol. 43, No. 2, P. 161–167
https://doi.org/10.1007/s13131-023-2261-z
http://www.aosocean.com
E-mail: ocean2@hyxb.org.cn

An improved algorithm based on equivalent sound velocity profile method at large incident angle

Qianqian Li[1, 2], Qian Tong[1], Fanlin Yang[1], Qi Li[1], Zhihao Juan[1], Yu Luo[1]*

[1] College of Geodesy and Geomatics, Shandong University of Science and Technology, Qingdao 266590, China

[2] College of Underwater Acoustic Engineering, Harbin Engineering University, Harbin 150001, China

Received 3 January 2023; accepted 21 August 2023

Abstract

With the development of ultra-wide coverage technology, multibeam echo-sounder (MBES) system has put forward higher requirements for localization accuracy and computational efficiency of ray tracing method. The classical equivalent sound speed profile (ESSP) method replaces the measured sound velocity profile (SVP) with a simple constant gradient SVP, reducing the computational workload of beam positioning. However, in deep-sea environment, the depth measurement error of this method rapidly increases from the central beam to the edge beam. By analyzing the positioning error of the ESSP method at edge beam, it is discovered that the positioning error increases monotonically with the incident angle, and the relationship between them could be expressed by polynomial function. Therefore, an error correction algorithm based on polynomial fitting is obtained. The simulation experiment conducted on an inclined seafloor shows that the proposed algorithm exhibits comparable efficiency to the original ESSP method, while significantly improving bathymetry accuracy by nearly eight times in the edge beam.

Key words: equivalent sound speed profile, ray tracing method, large incident angle, edge beam, deep sea, error correction, multibeam echo-sounder system

Citation: Li Qianqian, Tong Qian, Yang Fanlin, Li Qi, Juan Zhihao, Luo Yu. 2024. An improved algorithm based on equivalent sound velocity profile method at large incident angle. Acta Oceanologica Sinica, 43(2): 161–167, doi: 10.1007/s13131-023-2261-z

1 Introduction

Owing to the characteristics of high precision and wide coverage, high-resolution multibeam echo-sounder (MBES) system is an efficient acoustic approach for seafloor topography and geomorphology mapping, sediment characterisation and classification, and frequently applied in marine environmental management and mineral resource exploitation (de Moustier, 1986; Lamarche et al., 2011; Chen et al., 2019; Zhang et al., 2020). The MBES has been developed as a comprehensive device with an operation depth of up to 10–11 000 m and wide swath coverage of more than 140° at present (Farr, 1980; Wu et al., 2021; Zhao et al., 2021). For instance, the SeaBat T50-P MBES system of the Teledyne Reson Company has a large coverage angle of up to 170° (Teledyne Reson, 2022). The development of MBES ultra-wide coverage technology has further improved measurement efficiency. The depth and horizontal range of the beam impacting on the seafloor are initially calculated by the triangulation method which is based on the average sound velocity. However, due to the inhomogeneity of seawater, the sound velocity varies with temperature, salinity and water depth (Li et al., 2019). The temporal and spatial variation of sound velocity in seawater causes the refraction of sound waves, and the effective elimination of the refraction effect is essential to improve the accuracy of underwater acoustic localization (Červený et al., 1982; Wu et al., 2021). However, there is a tradeoff between bathymetry accuracy and computational quantity.

The sound velocity profile (SVP) is the vertical distribution of sound velocity with depth, and the seawater can be divided into multiple layers based on adjacent sound velocity observations. The ray tracing method employs ray theories to trace the propagation of the beams in combination with SVP (Zhao and Liu, 2008). Then the acoustic ray could be composed of many arcs under the assumption of a constant sound velocity gradient in each water layer, which approximates the practical propagation. Therefore, it tends to be highly accurate, but the abundant water layers resulting from high-density sound velocity values generate a great deal of calculation (Červený et al., 1982; Porter and Bucker, 1987). In contrast, the equivalent sound speed profile (ESSP) method requires only single-layer tracing and is free of complicated calculations. Because the position of beam footprint remains almost unchanged for a family of SVPs with the same surface value and integral area, a simple constant-gradient equivalent SVP can be utilized to replace the actual SVP (Geng and Zielinski, 1999). However, the ESSP is more efficient than the usual ray tracing method but less accurate (Jia et al., 2019). Notably, the positioning error of the ESSP method still increases with the incident angle and ocean depth, even at an accurate reference depth. The bathymetry accuracy of the edge beam (large incident angle) is often not within the 1% limit specified by the International Hydrographic Organization (International Hydro-

Foundation item: The Natural Science Foundation of Shandong Province of China under contract Nos ZR2022MA051 and ZR2020MA090; the National Natural Science Foundation of China under contract No. U22A2012; China Postdoctoral Science Foundation under contract No. 2020M670891; the SDUST Research Fund under contract No. 2019TDJH103; the Talent Introduction Plan for Youth Innovation Team in universities of Shandong Province (innovation team of satellite positioning and navigation).
*Corresponding author, E-mail: luoyu@sdust.edu.cn

graphic Organization, 2008), particularly in the deep-sea environment.

By analyzing the positioning error of the ESSP method at edge beam, it is discovered that the positioning error consistently increases with the incident angle. Therefore, empirical formula for error correction based on polynomial fitting was derived. The simulation experiment shows that the improved algorithm performs well with high accuracy and efficiency compared to the classical ESSP method.

2 Methods

2.1 *Ray tracing method*

The ray tracing method usually divides the water column into multiple layers and then obtain an accurate location by summing the depth and horizontal range of each individual layer. It is assumed for a certain layer i that the sound velocity varies linearly and the propagation of acoustic ray is a circular arc, as shown in Fig. 1. The sound velocity gradient g_i and radius R_i can be calculated by Eqs (1) and (2), respectively:

$$g_i = \frac{C_i - C_{i-1}}{\Delta z_i}, \tag{1}$$

$$R_i = -\frac{1}{pg_i}, \tag{2}$$

where $\Delta z_i = z_i - z_{i-1}$ is the layer thickness, C_{i-1} and C_i are adjacent sound velocities, θ_{i-1} is the incident angle.

The one-way travel time Δt_i and horizontal distance Δy_i in layer i can be obtained from Eqs (3) and (4), respectively:

$$\Delta t_i = \frac{1}{g_i} \ln\left[\frac{C_i(1+\cos\theta_{i-1})}{C_{i-1}(1+\cos\theta_i)}\right], \tag{3}$$

$$\Delta y_i = R_i(\cos\theta_i - \cos\theta_{i-1}) = \frac{[1-(pC_{i-1})^2)]^{1/2} - [1-p(C_{i-1}+g_i\Delta z_i)^2]^{1/2}}{pg_i}, \tag{4}$$

where p is the Snell constant and can be expressed as $p = \frac{\sin\theta_i}{C_i} = \frac{\sin\theta_0}{C_0}$ by Snell law.

According to the accumulated time T through the whole water column from Eq. (5), the depth Z and horizontal distance Y where the beam footprint is located can be deduced by Eq. (6):

$$T = \sum_{i=1}^{N} \Delta t_i, \tag{5}$$

$$Y = \sum_{i=1}^{N} \Delta y_i, \quad Z = \sum_{i=1}^{N} \Delta z_i. \tag{6}$$

2.2 *ESSP method*

In principle, the positioning accuracy of ray tracing method depends on the fineness of the SVP stratification. As the number of layers increases, the theoretically calculated acoustic ray will gradually approach the actual one. But it is followed by a significant amount of calculation. Hence, it is difficult to solve the conflict between positioning accuracy and computational complexity. Geng proposed that the position of beam footprint is only related to the initial incident angle θ_0, surface sound speed C_0 and SVP integrated area S_r with respect to the reference depth z_B. Thus, the actual SVP can almost be replaced by a constant-gradient SVP with the same surface value and integral area. The principle of the ESSP method is schematically illustrated in Fig. 2 (Geng and Zielinski, 1999).

Assuming that the integral area S_r of the actual SVP is the same as the equivalent SVP, the equivalent gradient g_{eq} and radius R_{eq} can be calculated as follows:

$$S_r = \frac{1}{2}(C_B + C_0)(z_B - z_0), \tag{7}$$

$$g_{eq} = \frac{C_B - C_0}{z_B - z_0} = \frac{2S_r}{(z_B - z_0)^2} - \frac{2C_0}{(z_B - z_0)}, \tag{8}$$

$$R_{eq} = \frac{-1}{pg_{eq}} = \frac{-C_0}{g_{eq}\sin\theta_0}, \tag{9}$$

According to ray theory and Eq. (10), the equivalent incident angle θ_{eq} at the reference depth z_B can be obtained from (Xin et al., 2018):

$$\theta_{eq} = 2\arctan(e^{g_{eq}t}\tan(\theta_0/2)). \tag{10}$$

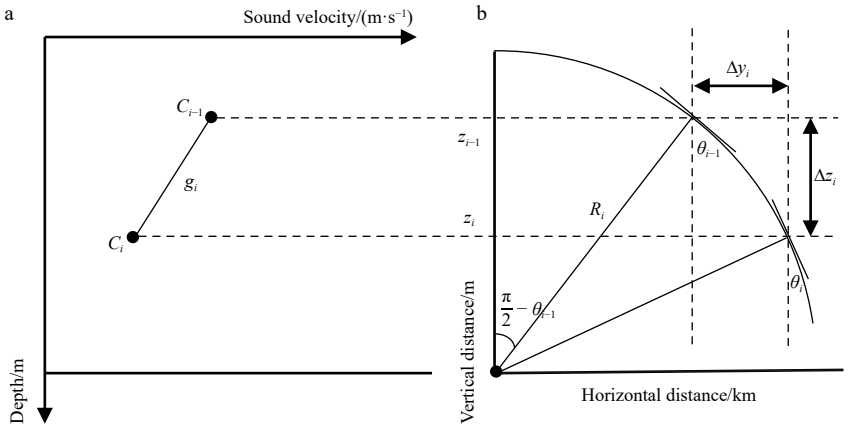

Fig. 1. Ray tracing method: the sound velocity (a) and the acoustic ray propagation trajectory (b) of the layer *i*.

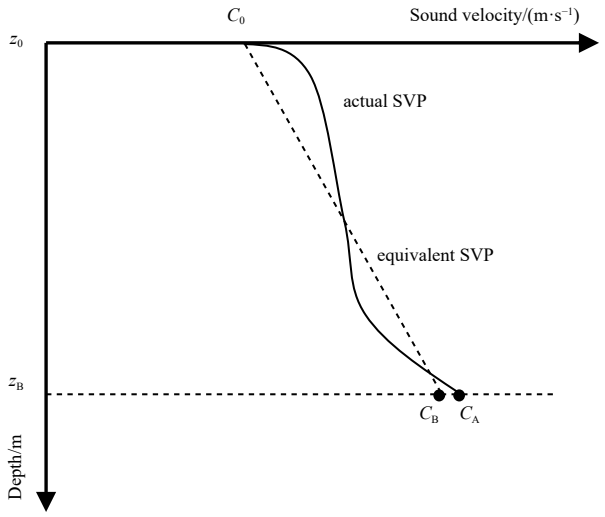

Fig. 2. The schematic diagram of the ESSP method, the solid line denotes the actual SVP ($C_0 - C_A$) and the dotted line denotes the equivalent SVP ($C_0 - C_B$).

Supposed that the beam is transmitted from z_0 and y_0 with an initial incident angle θ_0, and the measured one-way travel time is t, the position of the beam footprint can be calculated by Eq. (11):

$$\begin{cases} z_{eq} = z_0 + R_{eq}(\sin\theta_0 - \sin\theta_{eq}) = z_0 - \\ \qquad \dfrac{(\sin\theta_0 - \sin(2\arctan(e^{g_{eq}t}\tan(\theta_0/2))))}{pg_{eq}} \\ y_{eq} = y_0 + R_{eq}(\cos\theta_{eq} - \cos\theta_0) = y_0 - \\ \qquad \dfrac{(\cos(2\arctan(e^{g_{eq}t}\tan(\theta_0/2))) - \cos\theta_0)}{pg_{eq}} \end{cases}, \tag{11}$$

where (z_0, y_0) are the coordinates of the transducer array.

2.3 *Improved algorithm of the ESSP method*

2.3.1 *Error analysis for the ESSP method*

It has been proven that the relative depth error of the ESSP method is less than 0.1% in shallow water with depths shallower than 100 m (Geng and Zielinski,1999). However, the location accuracy of ESSP method for edge beam in deep water has not been discussed.

The SVP in Fig. 3a was measured by using the CTD in the South China Sea in 2019. It was assumed that there is a flat seafloor with a depth of 1 250 m, which is close to the average depth of the South China Sea. The initial incident angles of the MBES system are assumed to be 0°–80°, with an interval of 0.02°. When the SVP is sufficiently dense, the depth and horizontal distance calculated using the ray tracing method can be considered as true value.

To avoid the influence of reference depth error on the ESSP method, it is assumed that the reference depth is equal to the actual sea depth (1 250 m). Figures 3b and 3c illustrate the errors in depth and horizontal distance calculated using the ESSP method. The dotted line represents the 1% limit specified in the International Hydrographic Organization (IHO) Standards for Hydrographic Surveys Special Publication No.44 (Fig. 3b). It shows that both horizontal distance and depth errors increase with the incident angles. Especially when the incident angle exceeds 70°, the positioning errors of ESSP increase significantly with the angles, and the depth error exceeds the 1% limit. Therefore, "the large incident angle" is defined as the incident angle at which the depth error exceeds 1% of the actual depth. Figures 3b and c also show that the depth errors are positive, while the horizontal distance errors are negative. This suggests that the ESSP method yields shallower and more distant positioning results. In addition, it can be found that the error curve varies monotonically and regularity for large incident angle.

2.3.2 *Improved algorithm*

The previous section indicates that the positioning error of the edge beam increases monotonically with the incident angle. Therefore, we attempt to express the positioning error as a function of the incident angle by utilizing polynomial fitting. This positioning error can be used as a correction value to adjust the positioning results of the ESSP method.

The polynomial fitting function is usually expressed as:

$$\xi(\theta) = p_0 + p_1\theta + p_2\theta^2 + \cdots + p_m\theta^m, \tag{12}$$

where $\xi(\theta)$ is the fitted data, which can be regarded as the correction value of the proposed method, and θ is the initial incident angle (70°–80°). $p_i(i = 0, 1, \cdots, m)$ are the coefficients of the polynomial fitting function and n is the polynomial order. The depth error and horizontal distance error are defined by $\Delta_z(\theta)$

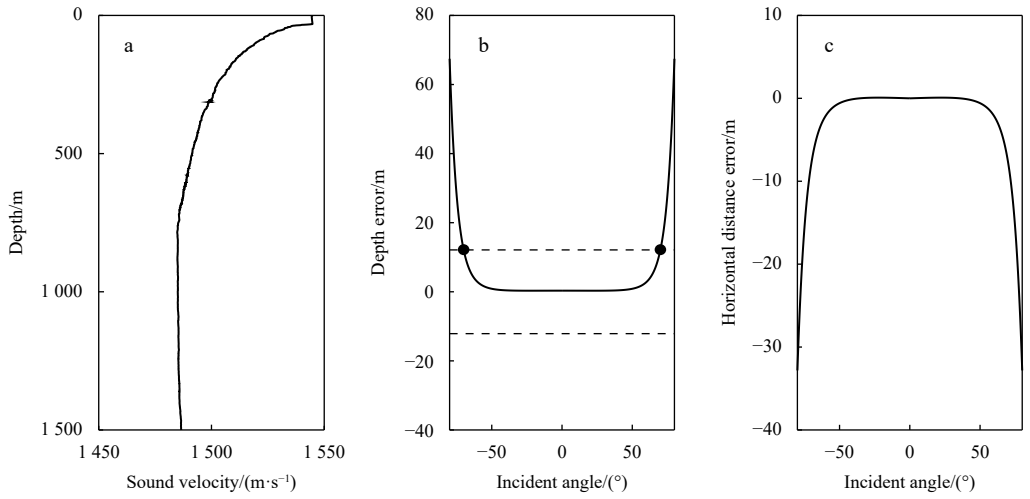

Fig. 3. The measured SVP (a). The position error of the ESSP method: the depth error (b) and horizontal distance error (c).

and $\Delta_y(\theta)$, respectively.

The least-squares method is used to define the most suitable function. The least-squares solution for polynomial coefficients $p_i(i=0,1,\cdots,m)$ is achieved through the minimization of the sum of squared errors $\delta_j^2=(\xi(\theta_j)-\Delta(\theta_j))^2, j=1,2,\cdots,n$, i.e., $Q=\underset{p_0,p_1,\cdots,p_m}{argmin}\sum_{j=1}^{n}\delta_j^2$ by the definition of least-squares fitting. It is speculated that the polynomial fitting order should be less than three because of unsophisticated variation of the error curve. Tables 1 and 2 show the coefficients of the 1-3 order polynomial fitting for the horizontal distance errors and depth errors, respectively.

Four evaluation indicators have been applied to assess the performance of fitted function as follows:

(1) The root mean square error (RMSE) is the square root of the sum of squares of the error between the fitted and original data. The smaller the value, the more stable is the fitted data.

(2) The mean absolute error (MAE) was used to evaluate the proximity between the fitted and original data.

(3) The coefficient of determination (R^2) reflected the accuracy of the fitted data. Generally, the range of R^2 is [0,1]. The closer the value is to 1, the better the fitting effect.

(4) The smaller the mean absolute percentage error (MAPE), the better is the fitting effect.

Table 1. Polynomial fitting coefficients for horizontal distance errors

	Linear	Quadratic	Cubic
Cubic coefficient			−0.009 5
Quadratic coefficient		−0.184 4	1.959 5
Monomial coefficient	−2.409 2	25.257 7	−135.395 7
Constant term coefficient	163.495 8	−872.469 8	3 136.691 6

Table 2. Polynomial fitting coefficients for depth errors

	Linear	Quadratic	Cubic
Cubic coefficient			0.028 1
Quadratic coefficient		0.469 3	5.848 9
Monomial coefficient	5.249 8	−65.146 5	4 082.955 1
Constant term coefficient	−3.618 8	2 274.045 6	−9 540.859 0

$$\mathrm{RMSE}=\sqrt{\frac{1}{N}\sum_{i=1}^{N}(\xi(\theta_i)-\Delta(\theta_i))^2}, \tag{13}$$

$$\mathrm{MAE}=\frac{1}{N}\sum_{i=1}^{N}|\xi(\theta_i)-\Delta(\theta_i)|, \tag{14}$$

$$R^2=1-\frac{\sum_{i=1}^{N}(\xi(\theta_i)-\Delta(\theta_i))^2}{\sum_{i=1}^{N}\left(\Delta(\theta_i)-\frac{1}{N}\sum_{i=1}^{N}\Delta(\theta_i)\right)^2}, \tag{15}$$

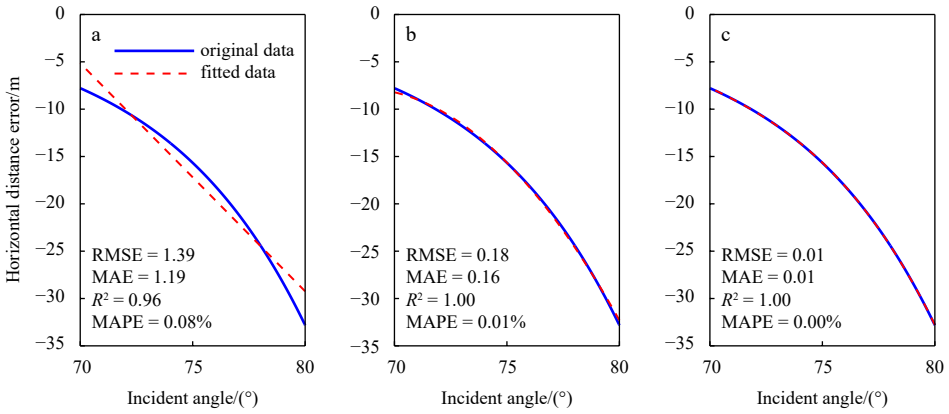

Fig. 4. Horizontal distance errors and their linear (a), quadratic (b), and cubic polynomial fitting (c).

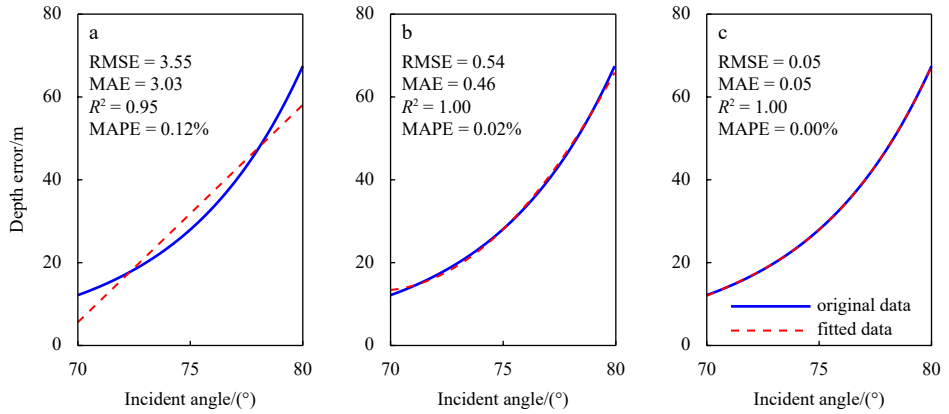

Fig. 5. Depth errors and their linear (a), quadratic (b), and cubic polynomial fitting (c).

$$\mathrm{MAPE} = \frac{1}{N}\sum_{i=1}^{N}\left(\frac{|\xi(\theta_i) - \Delta(\theta_i)|}{\Delta(\theta_i)}\right) \times 100\%, \tag{16}$$

where $\xi(\theta_i)$ is the fitted data and $\Delta(\theta_i)$ is the original data.

Considering that the positioning error curves of port side and starboard side in MBES are symmetric on the flat seafloor, only the positioning error on one side is discussed here. Figures 4 and 5 show the fitted curve and evaluation indicators of the horizontal distance and depth errors, respectively, which indicate that the RMSE and MAE evidently decrease with the fitting order. The R^2 values of the quadratic and cubic polynomial fitting are equal to 1, which is larger than the linear fitting. In addition, the MAPE of the quadratic and the cubic polynomial fitting are almost identical and larger than the linear fitting. In summary, quadratic and cubic polynomial fitting have similar performances, which perform significantly better than linear fitting.

The error correction values corresponding to an arbitrary large incident angle can be obtained by substituting coefficient into Eq. (12). Thus, the positioning results can be corrected by Eq. (17):

$$\begin{cases} Y_{\mathrm{corr}}(\theta_i) = y_{\mathrm{eq}}(\theta_i) + \xi_y(\theta_i) \\ Z_{\mathrm{corr}}(\theta_i) = z_{\mathrm{eq}}(\theta_i) + \xi_z(\theta_i) \end{cases}. \tag{17}$$

Since it is impossible to acquire the reference depth of each beam in advance, the bathymetry value of the central beam is generally used as the reference depth for all beams. According to the above description, the error correction values of the ESSP method at large incident angles based on the same reference depth on a flat seafloor can be obtained from a polynomial fitting in advance. The corrected positions are calculated by substituting error correction values into Eq. (17).

3 Results

3.1 *Applicability analysis*

The error analysis in section 2 is under the assumption that the reference depth is equal to the actual depth. However, in the case of highly uneven seafloor, the actual depths of the edge beams are often quite different from the reference depth (bathymetry value of the central beam), leading to substantial errors in the calculation of the beam footprint position. Therefore, in order to evaluate the adaptability and performance of the improved algorithm, it is necessary to analyze the situation when the reference depth (1 250 m) is inconsistent with the actual depth (1 000–1 500 m).

Figure 6 illustrates the depth errors of the classical ESSP method and the improved algorithm, with the black dashed box representing the region where the bathymetry values within the accuracy. The depth accuracy is defined by the IHO for a 1% of water depth. It indicates that only 15.98% of bathymetry values of the ESSP method meet the 1% water depth limit. However, after error correction using the correction values obtained by quadratic and cubic polynomial fitting respectively, the proportion of bathymetry values meeting the accuracy requirement are increased to 71.97% and 72.32%. For the edge beam with an incident angle of 80°, Fig. 6b shows that the bathymetry value meets the accuracy requirement when the actual depth is 1 180–1 335 m, and Fig. 6c shows that the bathymetry value meets the accuracy requirement when the actual depth is 1 169–1 327 m. It can be seen that the positioning performance in Figs. 6b and Fig. 6c is very similar. Considering the efficiency of polynomial fitting, the quadratic polynomial fitting method is chosen to obtain the error correction values in this paper. Therefore, the error correction value can be determined by the following equations:

$$\begin{cases} \xi_{\mathrm{y}}(\theta_i) = p_{y0} + p_{y1}\theta_i + p_{y2}\theta_i^2, \\ \xi_{\mathrm{z}}(\theta_i) = p_{z0} + p_{z1}\theta_i + p_{z2}\theta_i^2. \end{cases} \tag{18}$$

3.2 *Performance in the inclined seafloor*

To further verify the adaptability performance, an inclined seafloor with a slope angle of 1° is assumed, as shown in Fig. 7. The MBES coverage angles range from –80° to +80°. The position where the transducer array lie is assumed to be the origin of the coordinates. The *Y*-axis is perpendicular to the bow and stern, pointing towards the starboard side, and the *Z*-axis points to the seafloor perpendicularly. The water depth directly below the transducer is 1 250 m, which serves as the reference depth for each beam. The SVP is shown in Fig. 3a.

As shown in Fig. 8, the coordinates of the beam footprint are calculated by the ray tracing method, ESSP method and proposed algorithm, respectively. It can be seen that for the beam with small incident angles, the bathymetry accuracy of the three methods is almost equivalent. As the incident angle increases, the relative depth errors of the ESSP method become much larger, and the edge beam no longer meet the 1% water depth limit. For the port edge beam, the maximum horizontal distance error and depth error are 42.72 m and 80.49 m respectively, and the relative depth error is 6.8%. For the starboard edge beam, the maximum horizontal distance error and depth error are –20.58 m and 52.9 m respectively, and the relative depth error is 4%. In contrast, the bathymetry accuracy of the improved algorithm for

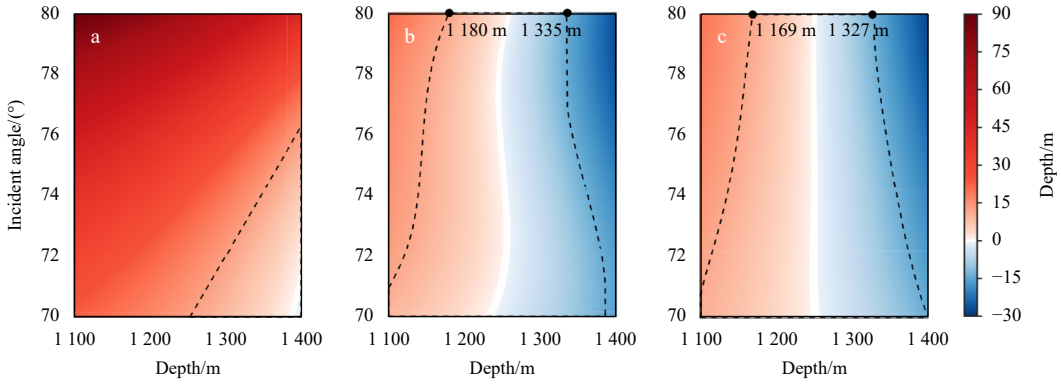

Fig. 6. Depth errors calculated by the ESSP method (a), proposed methods after quadratic (b) and cubic polynomial fitting (c).

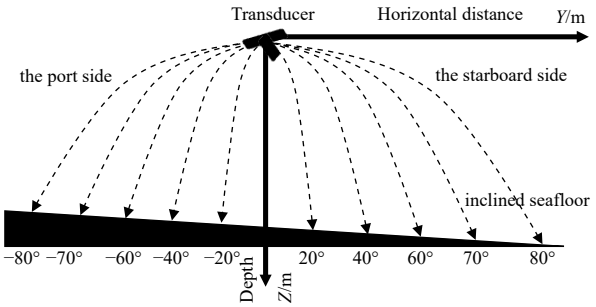

Fig. 7. Inclined seafloor topography and coordinate axis setting.

edge beam is much better than that of the ESSP method, and the horizontal distance errors and depth errors of the port and starboard side edge beam are significantly reduced (as shown in red font in Fig. 8). The maximum relative depth error of the port side is 0.96%, and that of the starboard side is –0.86%, both of which meet the requirement of 1% water depth accuracy.

Figure 8 also shows that the bathymetry results of the improved algorithm on the port edge are shallower, while the bathymetry results on the starboard edge are deeper than the true depth. To further explain the above phenomenon, the bathymetry errors of the three methods in Fig. 6 with the incident angle when the actual depth is 1 100 m and 1 400 m respectively are shown in Fig. 9.

Figure 9a illustrates the bathymetry error with the incident angle when the actual depth is 1 100 m, which can represent the situation when the reference depth is greater than the actual depth. It can be seen that the depth error of ESSP method is greater than the error correction value, so the corrected bathymetry result is still shallower than the actual depth. This demonstrates that the improved algorithm has the problem of undercorrection when the actual depth is less than the reference depth. Figure 9b illustrates the bathymetry error with the incident angle when the actual depth is 1 400 m, which can represent the situ-

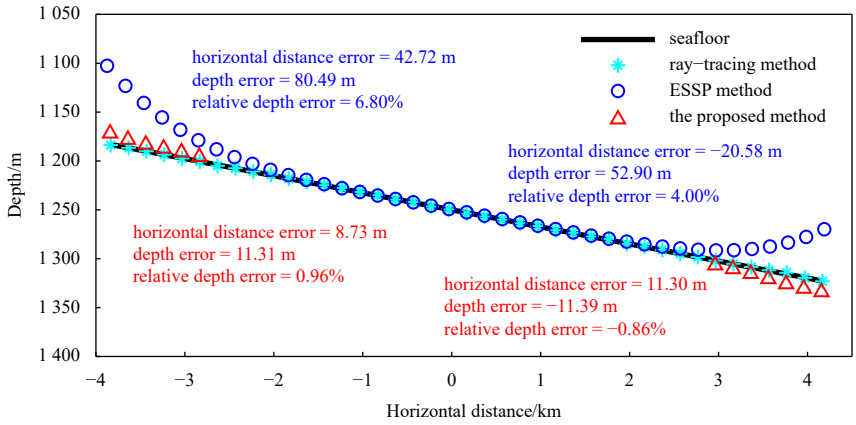

Fig. 8. Beam footprint coordinates calculated by the ray tracing method, ESSP method, and the proposed method.

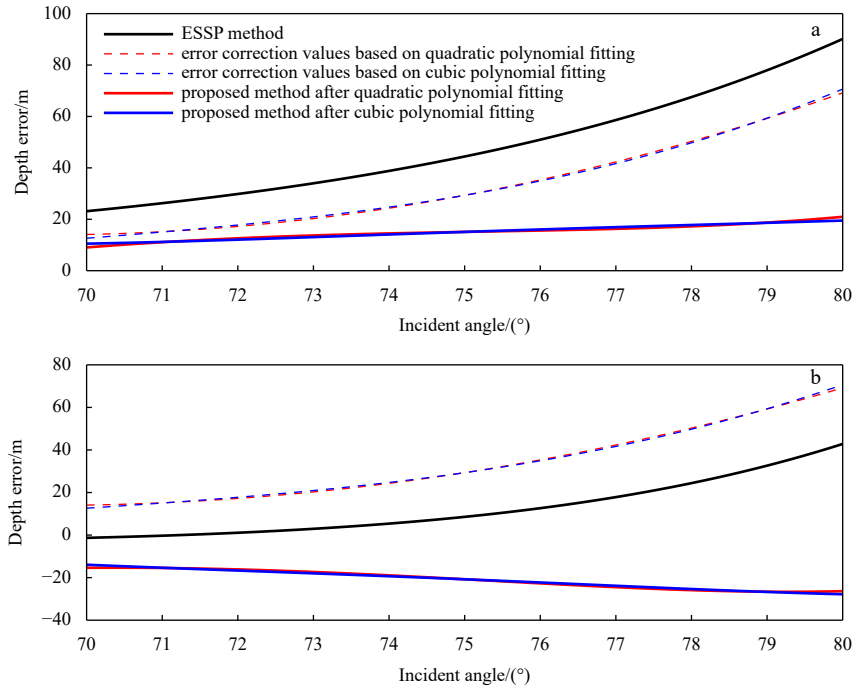

Fig. 9. Depth error calculated by ESSP method, proposed methods after quadratic and cubic polynomial fitting at actual depths of 1 100 m (a) and 1 400 m (b) and error correction values at actual depth of 1 250 m.

ation when the reference depth is smaller than the actual depth. It can be seen that since the bathymetry error of ESSP method is less than the error correction value, the improved algorithm overcorrects the depth error, and the corrected bathymetry is deeper than the actual depth.

In general, although the positioning accuracy of the improved algorithm is lower at large incident angles, it is still significantly higher than that of the ESSP method, and the bathymetry accuracy can meet the requirement of 1% depth accuracy in the inclined seafloor with a gentle slope.

In order to analyze the computational efficiency of different algorithms, 100 beam footprint positions are carried out by the ray tracing method, ESSP method, and proposed method in this paper respectively, and the average running time is shown in Table 3. It indicates that the ray tracing method has the lowest computational efficiency, and the average calculation time is 0.058 2 s, the average calculation time of ESSP method and the improved algorithm in this paper is 0.000 8 s and 0.000 9 s, respectively. It can be seen that the computational efficiency of the improved algorithm is close to that of the ESSP method, but significantly higher than that of the ray tracing method.

Table 3. The average computation time of 100 calculations

	Ray tracing method	ESSP method	Proposed method
Time/s	0.058 2	0.000 8	0.000 9

4 Conclusions

When processing multibeam bathymetry data, the ESSP method can obtain relatively accurate bathymetry results efficiently in shallow water environment. However, the positioning accuracy of the ESSP method is substantially limited for the edge beams in deep sea. Therefore, an improved algorithm based on quadratic polynomial fitting is proposed. On the basis of analyzing the positioning error of ESSP method, the improved algorithm obtains the error correction by polynomial fitting. Simulation results show that the improved algorithm can achieve accurate positioning under inclined seafloor, the relative depth error is less than 1%, and the positioning accuracy is comparable to the ray tracing method, and has higher computational efficiency. However, due to the inconsistency between the reference depth and the actual depth, the improved algorithm may be under-corrected or over-corrected when the seafloor is very rough. In future work, a more accurate reference depth will be obtained through an equivalent sound speed iterative method to reduce errors associated with a single reference depth.

References

Červený V, Popov M M, Pšenčík I. 1982. Computation of wave fields in inhomogeneous media - Gaussian beam approach. Geophysical Journal International, 70(1): 109–128, doi: 10.1111/j.1365-246X.1982.tb06394.x

Chen Yilan, Ding Jisheng, Zhang Haiquan, et al. 2019. Multibeam water column data research in the Taixinan Basin: Implications for the potential occurrence of natural gas hydrate. Acta Oceanologica Sinica, 38(5): 129–133, doi: 10.1007/s13131-019-1444-0

de Moustier C. 1986. Beyond bathymetry: Mapping acoustic backscattering from the deep seafloor with Sea Beam. The Journal of the Acoustical Society of America, 79(2): 316–331, doi: 10.1121/1.393570

Farr H K. 1980. Multibeam bathymetric sonar: sea beam and hydro chart. Marine Geodesy, 4(2): 77–93, doi: 10.1080/15210608009379375

Geng Xueyi, Zielinski A. 1999. Precise multibeam acoustic bathymetry. Marine Geodesy, 22(3): 157–167, doi: 10.1080/014904199273434

International Hydrographic Organization. 2008. Special Publication 44. IHO Standards for Hydrographic Surveys. 5th ed. Monaco: International Hydrographic Bureau, 14–16.

Jia Yuqing, Su Lin, Mo Yaxiao, et al. 2019. A method of constructing equivalent sound speed profile in complex shallow water. Journal of Applied Acoustics (in Chinese), 38(4): 623–634, doi: 10.11684/j.issn.1000-310X.2019.04.020

Lamarche G, Lurton X, Verdier A L. 2011. Quantitative characterisation of seafloor substrate and bedforms using advanced processing of multibeam backscatter—Application to Cook Strait, New Zealand. Continental Shelf Research, 31(S2): S93–S109, doi: 10.1016/j.csr.2010.06.001

Li Qianqian, Shi Juan, Li Zhenglin, et al. 2019. Acoustic sound speed profile inversion based on orthogonal matching pursuit. Acta Oceanologica Sinica, 38(11): 149–157, doi: 10.1007/s13131-019-1505-4

Porter M B, Bucker H P. 1987. Gaussian beam tracing for computing ocean acoustic fields. The Journal of the Acoustical Society of America, 82(4): 1349–1359, doi: 10.1121/1.395269

Teledyne Reson. 2022. SeaBat T50-P product leaflet. https://www.teledynemarine.com/en-us/products/SiteAssets/RESON/SeaBat%20T50-P%20product%20leaflet.pdf[2022-12-22]

Wu Ziyin, Yang Fanlin, Tang Yong. 2021. Multi-beam bathymetric technology. In: Wu Ziyin, Yang Fanlin, Tang Yong, eds. High-resolution Seafloor Survey and Applications. Singapore: Springer, 21–76, doi: 10.1007/978-981-15-9750-3_2

Xin Mingzhen, Yang Fanlin, Wang Faxing, et al. 2018. A TOA/AOA underwater acoustic positioning system based on the equivalent sound speed. The Journal of Navigation, 71(6): 1431–1440, doi: 10.1017/S037346331800036X

Zhang Kai, Li Qianqian, Zhu Hongchun, et al. 2020. Acoustic deep-sea seafloor characterization accounting for heterogeneity effect. IEEE Transactions on Geoscience and Remote Sensing, 58(5): 3034–3042, doi: 10.1109/TGRS.2019.2946986

Zhao Jianhu, Liu Jingnan. 2008. Multi-Beam Sounding and Image Data Processing (in Chinese). Wuhan: Wuhan University Press, 124–142

Zhao Dineng, Wu Ziyin, Zhou Jieqiong, et al. 2021. From 10 m to 11000 m, automatic processing multi-beam bathymetric data based on PGO method. IEEE Access, 9: 14516–14527, doi: 10.1109/ACCESS.2021.3051909